

Numerical Relativity at the Frontier

Stuart L. SHAPIRO

*Departments of Physics and Astronomy, University of Illinois at
Urbana-Champaign*

Loomis Laboratory, 1110 West Green Street, Urbana, IL 61801

Numerical relativity is an essential tool for solving Einstein's equations of general relativity for dynamical systems characterized by high velocities and strong gravitational fields. The implementation of new algorithms that can solve these nonlinear equations in $3 + 1$ dimensions has enabled us to tackle many long-standing problems of astrophysical interest, leading to an explosion of important new results. Numerical relativity has been used to simulate the evolution of a diverse array of physical systems, including coalescing black hole and neutron star binaries, rotating and collapsing compact objects (stars, collisionless clusters, and scalar fields), and magnetic and viscous stars, to name a few. Numerical relativity has been exploited to address fundamental points of principle, including critical phenomena and cosmic censorship. It holds great promise as a guide for interpreting observations of gravitational waves and gamma-ray bursts and identifying the sources of such radiation. Highlights of a few recent developments in numerical relativity are sketched in this brief overview.

§1. Introduction

General relativity—Einstein's theory of relativistic gravitation—is the cornerstone of modern cosmology, the physics of neutron stars and black holes, the generation of gravitational radiation, and countless other cosmic phenomena in which strong-field gravitation is believed to play a dominant role. However solutions to Einstein's equations, except for a few idealized cases characterized by high degrees of symmetry, have not been obtained as yet for many of the important dynamical scenarios thought to occur in nature. Only now, with the advent of supercomputers, is it possible to tackle these highly nonlinear equations numerically and to explore these scenarios in detail. That is the main goal of numerical relativity, the art and science of developing computer algorithms to solve Einstein's equations for physically realistic, high-velocity, strong-field systems. Numerical relativity also has a pressing goal—to calculate gravitational waveforms from promising astrophysical sources, in order to provide theoretical templates both for the new ground-based gravitational-wave laser interferometers like LIGO in the US, VIRGO in Italy, GEO in Germany, and TAMA in Japan, as well as for space-based interferometers such as LISA, now being planned in the US, Europe and Japan.

This paper is a brief summary of a few recent developments in numerical relativity. It is far from complete and undoubtedly subject to my personal tastes and preferences. For example, my own short list of the 'hottest' topics in the field currently consists of the following:

- Binary black holes (BBHs)
- Binary neutron stars (BNSs)
- Binary black hole-neutron stars (BBHNSs)

- Rotating relativistic stars
- Collisionless clusters
- Scalar fields
- Critical phenomena
- Cosmic censorship
- General relativistic magnetohydrodynamics (GRMHD)

The inspiral and coalescence of BBHs, BNSs and BBHNSs top the list, as they represent the most likely sources of gravitational waves for detection by the laser interferometers [See Ref. 1) for a recent review and references and Refs. 2)–4) for important updates]. BNSs and BBHNSs are also strong candidates for short-period gamma-ray burst sources. Numerical relativity is crucial for constructing astrophysically realistic initial configurations of relativistic binaries in close, quasiequilibrium, nearly circular orbits, as well as for tracking their subsequent inspiral and merger. In the case of fluid star companions, the equations of relativistic hydrodynamics must be integrated together with Einstein’s gravitational field equations. Numerical relativity is also important in the study of rotating, relativistic stars, especially NSs. Gravitational collapse, the dynamical evolution of stars subject to nonaxisymmetric instabilities (like the dynamical bar-mode instability^{5),6)} and the secular evolution of stars driven by viscosity,⁷⁾ are all being explored by numerical simulations. Collisionless matter obeying the relativistic Vlasov equation has been treated in depth using the tools of numerical relativity.^{8)–10)} For example, binary clusters of collisionless particles that undergo collapse prior to merger have been used to simulate head-on collisions of binary black holes¹¹⁾ and the results have been useful in probing the geometry of coalescing event horizons.¹²⁾ Scalar fields have been employed as matter sources to study wave propagation, collapse,¹³⁾ critical phenomena^{14),15)} and binary BHs.⁴⁾ In the course of all of these numerical simulations, questions of fundamental physics have been addressed, including critical phenomena and cosmic censorship.¹⁶⁾ One of the latest thrusts, general relativistic magnetohydrodynamics (GRMHD) in dynamical spacetimes, promises to probe some of the astrophysically most important, unsolved aspects of magnetized stars and disks in strong gravitational fields.^{17)–20)}

In the sections below I will sketch results of some recent work on several of the topics described above. My emphasis will be on astrophysical systems that involve strong gravitational fields coupled to relativistic matter sources. My goal is not to record final, definitive solutions but rather to convey the flavor and breadth of current activity and the extent to which the latest algorithms and computational machinery now make it possible to obtain definitive solutions.

§2. 3+1 Formalism

Most current work in numerical relativity is performed within the framework of the 3 + 1 decomposition of Einstein’s field equations using some adaptation of the standard ADM equations.²¹⁾ In this framework spacetime is sliced up into a sequence of spacelike hypersurfaces of constant time t , appropriate for solving an

initial-value problem. Consider two such time slices separated by an infinitesimal interval dt as shown in Fig 1. The spacetime metric gives the invariant interval

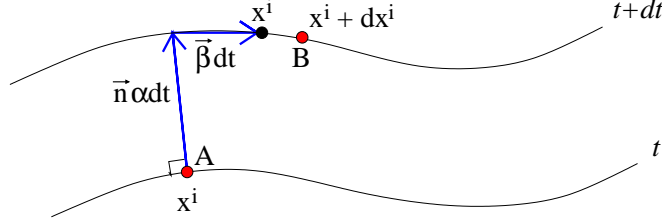


Fig. 1. 3+1 decomposition of spacetime.

between neighboring points A and B on the two slices according to

$$ds^2 = -\alpha^2 dt^2 + \gamma_{ij}(dx^i + \beta^i dt)(dx^j + \beta^j dt) , \quad (2.1)$$

where γ_{ij} is the 3-metric on a time slice, α is the lapse function determining the proper time between the slices as measured by a time-like normal observer n^a at rest in the slice, and β^i is the shift, a spatial 3-vector that describes the relabeling of the spatial coordinates of points in the slice. The gravitational field satisfies the Hamiltonian and momentum *constraint equations* on each time slice, including the initial slice at $t = 0$:

$$R + K^2 - K_{ij}K^{ij} = 16\pi\rho \quad (\text{Hamiltonian}) , \quad (2.2)$$

$$D_j(K^{ij} - \gamma^{ij}K) = 8\pi S^i \quad (\text{momentum}) . \quad (2.3)$$

Here $R = R^i_i$ is the scalar curvature on the slice, R_{ij} is the 3-Ricci tensor, K_{ij} is the extrinsic curvature, K is its trace, and D_j is the covariant derivative operator on the slice. The quantities ρ and S^i are the mass and momentum densities of the matter, respectively; such matter source terms are formed by taking suitable projections of the matter stress-energy tensor T^{ab} with respect to the normal observer.

A gravitational field satisfying the constraint equations on the initial slice can be determined at future times by integrating the *evolution equations*,

$$\partial_t \gamma_{ij} = -2\alpha K_{ij} + D_i \beta_j + D_j \beta_i , \quad (2.4)$$

$$\partial_t K_{ij} = \alpha(R_{ij} - 2K_{ik}K^k_j + KK_{ij}) - D_i D_j \alpha \quad (2.5)$$

$$+ \beta^k \partial_k K_{ij} + K_{ik} \partial_j \beta^k + K_{kj} \partial_i \beta^k - 8\pi\alpha(S_{ij} - \frac{1}{2}\gamma_{ij}(S - \rho)) ,$$

where S and S_{ij} are additional matter source terms. The evolution equations guarantee that the field equations will automatically satisfy the constraints on all future time slices identically, provided they satisfy them on the initial slice. Of course, this statement applies to the analytic set of equations and not necessarily to their numerical counterparts.

Note that the 3 + 1 formalism prescribes no equations for α and β^i . These four functions embody the four-fold gauge (coordinate) freedom inherent in general relativity. Choosing them judiciously, especially in the presence of black holes, is one of the main challenges of numerical relativity.

2.1. The BSSN Scheme

During the past decade, significant improvement in our ability to numerically integrate Einstein's equations stably in full 3 + 1 dimensions has been achieved by recasting the original ADM system of equations. One such reformulation is the so-called BSSN scheme.²²⁾ In this scheme, the physical metric and extrinsic curvature variables are replaced in favor of the conformal metric and extrinsic curvature, in the spirit of the ‘‘York-Lichnerowicz’’ split.²³⁾

$$\tilde{\gamma}_{ij} = e^{-4\phi} \gamma_{ij}, \quad \text{where} \quad e^{4\phi} = \gamma^{1/3}, \quad (2.6)$$

$$\tilde{A}_{ij} = \tilde{K}_{ij} - \frac{1}{3} \tilde{\gamma}_{ij} K. \quad (2.7)$$

Here a tilde $\tilde{}$ denotes a conformal quantity and γ is the determinant of γ_{ij} . At the same time, a connection function $\tilde{\Gamma}^i$ is introduced according to

$$\tilde{\Gamma}^i \equiv \tilde{\gamma}^{jk} \tilde{\Gamma}^i_{jk} = -\partial_j \tilde{\gamma}^{ij}. \quad (2.8)$$

The quantities that are independently evolved in this scheme are now $\tilde{\gamma}_{ij}$, \tilde{A}_{ij} , ϕ , K and $\tilde{\Gamma}^i$. The advantage is that the Riemann operator appearing in the evolution equations (cf. eqn. (2.5)) takes on the form,

$$\tilde{R}_{ij} = -\frac{1}{2} \underbrace{\tilde{\gamma}^{lm} \partial_m \partial_l \tilde{\gamma}_{ij}}_{\text{‘Laplacian’}} + \underbrace{\tilde{\gamma}_{k(i} \partial_j) \tilde{\Gamma}^k}_{\text{remaining 2nd deriv}} + \dots. \quad (2.9)$$

Thus the principal part of this operator, $\tilde{\gamma}^{lm} \partial_m \partial_l \tilde{\gamma}_{ij}$ is that of a Laplace operator acting on the components of the metric $\tilde{\gamma}_{ij}$. All the other second derivatives of the metric have been absorbed in the derivatives of the connection functions. The coupled evolution equations for $\tilde{\gamma}_{ij}$ and \tilde{A}_{ij} (cf. eqns. (2.4) and (2.5)) then reduce essentially to a wave equation,

$$\partial_t^2 \tilde{\gamma}_{ij} \sim \partial_t \tilde{A}_{ij} \sim \tilde{R}_{ij} \sim \nabla^2 \tilde{\gamma}_{ij}. \quad (2.10)$$

Wave equations not only reflect the hyperbolic nature of general relativity, but can be implemented numerically in a straight-forward and stable manner. By now, numerous simulations have demonstrated the dramatically improved stability achieved in the BSSN scheme over the standard ADM equations, and considerable effort has gone into explaining the improvement on theoretical grounds [see Ref. 1) for references].

§3. Code Testing

Much of the life of a computational relativist is devoted to code verification. This essential aspect of numerical relativity combines physical and mathematical insight with dedication and fortitude. Code verification takes on diverse forms. For example, one component consists of *convergence testing* to check that as the numerical spacetime lattice is shrunk to smaller scale to achieve higher resolution, the

integrations converge to a unique solution in a manner consistent with the order of truncation of the numerical scheme. Another component involves either identifying, or deriving from scratch, exact solutions, and then *reproducing exact solutions numerically*. In the case of vacuum spacetimes such test-bed solutions might consist of linearized, propagating gravitational waves and stationary black holes. In the case of spacetimes containing hydrodynamic fluid sources, typical test-bed solutions consist of shocks (e.g., the relativistic Riemann problem), nonrotating and rotating stars in stable equilibrium, and spherical, homogeneous dust-ball collapse to a black hole (Oppenheimer-Snyder collapse) expressed in various gauges. For spacetimes involving general relativistic magnetohydrodynamics, MHD wave propagation and MHD shocks, and the excitation of MHD waves by linearized gravitational waves, all yield exact solutions that serve as useful debugging tools.

Monitoring constraint violation is another mandatory aspect of code validation for a dynamical simulation. Not only must the fundamental Hamiltonian and momentum constraints, eqns. (2.2) and (2.3), be satisfied to some specified numerical tolerance at all times during a simulation, but any additional constraints associated with the adopted formalism must also be obeyed. In BBSN, for example, the quantities $\tilde{\gamma}_{ij}$ and \tilde{T}^i are separately evolved, hence the definition (2.8) emerges as a constraint. For GRMHD simulations, it is crucial to satisfy the magnetic field constraint equation, $D_i B^i = 0$.

Finally, *monitoring global conserved quantities* during a dynamical simulation provides an additional diagnostic tool. Useful diagnostics include the total (ADM) mass-energy M , the linear momentum P^i and the angular momentum J^i of the system, allowing for any energy and momentum carried off the computational grid by an outgoing flux of gravitational waves, matter and other forms of radiation. Other useful conserved quantities include the rest-mass M_0 when matter is present, and diagnostics like fluid circulation \mathcal{C} in adiabatic hydrodynamic flow (Kelvin's theorem).

§4. Binary Neutron Star Mergers and Hypermassive Stars

The protagonist of several different astrophysical scenarios probed by recent numerical simulations is a hypermassive star, typically a hypermassive neutron star. A hypermassive star is an equilibrium fluid configuration that supports itself against gravitational collapse by *differential* rotation. Uniform rotation can increase the maximum mass of a nonrotating, spherical equilibrium (TOV) star by at most $\sim 20\%$, but differential rotation can achieve a much higher increase.^{5),25)} Dynamical simulations demonstrate²⁴⁾ that hypermassive stars can be constructed that are *dynamically* stable, provided the ratio of rotational kinetic to gravitational potential energy, β , is not too large; for $\beta \gtrsim 0.24$ the configuration is subject to a nonaxisymmetric dynamical bar instability.^{5),6)} However, all hypermassive stars are *secularly* unstable to the redistribution of angular angular momentum by viscosity, magnetic braking or turbulence, or any other agent that dissipates internal shear. Such a redistribution tends to drive a hypermassive star to uniform rotation, which cannot support the mass against collapse. Hence hypermassive stars are transient phenom-

ena. Their formation following, for example, the merger of the neutron stars in a binary, or core collapse in a massive, rotating star, may ultimately lead to a ‘delayed’ collapse to a black hole on secular (dissipative) timescales. Such a collapse will be accompanied inevitably by a delayed gravitational wave burst.²⁴⁾

The above scenario has become very relevant in light of the most recent and detailed simulations of binary neutron star mergers in full general relativity. Dynamical simulations begin with initial data constructed to approximate astrophysically realistic binaries in quasistationary circular orbits at close separation. To construct such data, the initial value (constraint) equations (2.4) and (2.5) are solved for the metric via the conformal thin-sandwich approximation,²⁶⁾ where quasistationarity in the rotating frame of the binary is imposed by assuming that the spacetime is endowed with a helical Killing vector. The initial spatial metric is often assumed to be conformally flat. The initial matter profile is obtained by integrating the Euler equation together with the constraints. Two extreme opposite limits account for the stellar spins: corotational²⁷⁾ and irrotational binaries.²⁸⁾ Irrotational binary stars are physically more realistic for BNSs, since there is insufficient time for viscosity to achieve corotation prior to merger.²⁹⁾

State-of-the-art, fully relativistic simulations of BNSs have been performed by Shibata and his collaborators. They consider mergers of $n = 1$ polytropes,³⁰⁾ as well as configurations obeying a realistic nuclear equation of state (EOS).²⁾ They treat mass ratios Q_M in the range $0.9 \leq Q_M \leq 1$, consistent with the range of Q_M in observed binary pulsars with accurately determined masses.³¹⁾ The key result is that there exists a critical mass $M_{\text{crit}} \sim 2.5 - 2.7M_\odot$ of the binary system above which the merger leads to prompt collapse to a black hole, and below which the merger forms a hypermassive remnant. The hypermassive remnant undergoes delayed collapse in about ~ 100 ms and emits a delayed gravitational wave burst. Most interesting, prior to collapse, the remnant forms a triaxial bar when a realistic EOS is adopted (see Fig. 2) and the bar emits quasiperiodic gravitational waves at a frequency $f \sim 3 - 4$ kHz. Such a signal may be detectable by Advanced LIGO. It is interesting that for the adopted EOS, the mass M_{crit} is close to the value of the total mass found in each of the observed binary pulsars. Given that the masses of the individual stars in a binary can be determined by measuring the gravitational wave signal emitted during the adiabatic, inspiral epoch prior to plunge and merger, the detection (or absence) of any quasiperiodic emission from the hypermassive remnant prior to delayed collapse may significantly constrain models of the nuclear EOS.

The possibility of a hypermassive neutron star remnant formed following a BNS merger had been foreshadowed in earlier Newtonian simulations,³²⁾ post-Newtonian simulations³³⁾ and conformally flat general relativistic simulations.³⁴⁾ However, the recent fully relativistic simulations reported in Ref. 2) provide the strongest theoretical evidence to date, although the details undoubtedly depend on the adopted EOS. Triaxial equilibria can arise only in stars that can support sufficiently high values of β exceeding the classical bifurcation point at $\beta \approx 0.14$; reaching such high values requires EOSs with adiabatic indices exceeding $\Gamma \approx 2.25$ in Newtonian configurations, and comparable values in relativistic stars. It is not yet known whether the true nuclear EOS in neutron stars is this stiff, or what agent for redistributing an-

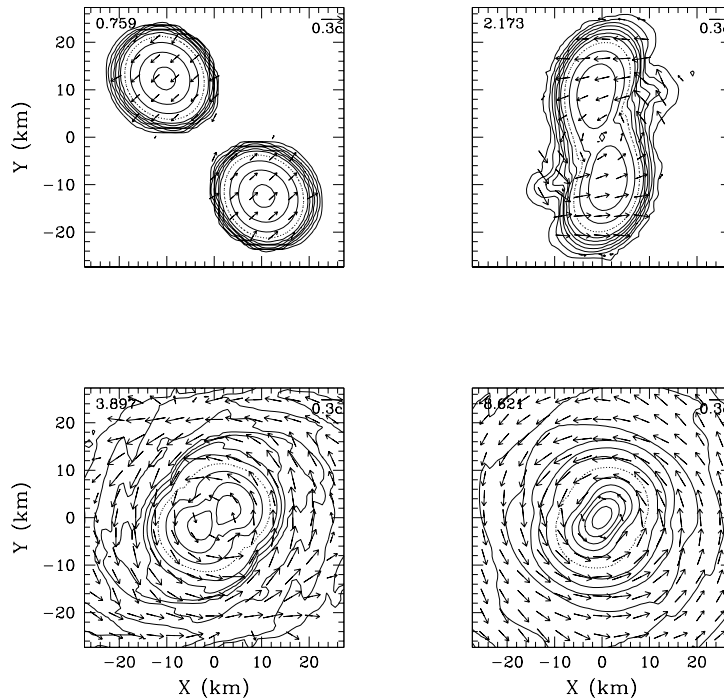


Fig. 2. Formation of triaxial hypermassive remnant following BNS merger in $2.7M_{\odot}$ system. Snapshots of density contours are shown in the equatorial plane. The number in the upper left-hand corner denotes the elapsed time in ms; the initial orbital period is 2.11 ms. Vectors indicate the local velocity field. [From Shibata, Taniguchi and Uryu 2005.]

gular momentum in a hypermassive star dominates (e.g., magnetic fields, turbulent viscosity or gravitational radiation). But it is already evident that hypermassive stars are likely to form from some mergers and that they will survive many dynamical timescales before undergoing delayed collapse. The recent measurement³⁵⁾ of the mass of a neutron star in a NS-white dwarf binary of $M_{\odot} = 2.1$ establishes an observational lower limit for the maximum mass of a neutron star; such a high value suggests that mergers in typical BNSs may form hypermassive stars more often than undergoing prompt collapse.

§5. Black Hole Excision

The challenge of simulating a black hole numerically is avoiding encountering the spacetime singularity inside the hole. Failure to do so results in infinities that cause the numerical integrations to terminate. While suitable gauge conditions can postpone the appearance of singularities, they are susceptible to “grid stretching” inaccuracies that usually infect the metric near the horizon and grow with time; see Ref. 1) for discussion and Fig. 7 in Section 8 for an example. One of the most promising new methods of dealing with black hole singularities is black hole excision. This

method, first suggested by Unruh,³⁶⁾ exploits the fact that the singularity resides inside an event horizon, a region that is casually disconnected from the rest of the universe. Since no physical information propagates from inside the event horizon to outside, one should be able to evolve the exterior independent of the interior space-time. Inside the event horizon, causality entitles us to do almost “anything” which will produce a stable exterior evolution. In particular, one can excise the computational domain inside the horizon and replace it with suitable boundary conditions at its outer surface.

Although it is guaranteed that no physical signal can propagate from inside the horizon to outside, unphysical signals often can propagate in evolution codes. Gauge modes can move acausally for many gauge conditions. Although they carry no physical content, such modes may destabilize the code. Thus, the choice of gauge is crucial to obtaining good post-excision evolutions. In addition, constraint-violating modes can, for some formulations of the field equations, propagate acausally, creating inaccuracies and instabilities. Thus, the choice of formulation is also crucial to obtaining good post-excision evolutions.

The feasibility of black hole excision was first demonstrated in spherically symmetric 1+1 dimensional evolutions of a single black hole in the presence of a self-gravitating scalar field.^{13),37)} Excision was also implemented early on to study the spherically symmetric collapse of collisionless matter to a black hole in Brans-Dicke theory.³⁸⁾ Full 3 + 1 evolutions of vacuum black hole spacetimes were attempted with excision using the standard ADM formulation, both for a stationary³⁹⁾ and for a boosted black hole.⁴⁰⁾ Although the introduction of excision improved the behavior of these black hole simulations, long-term stability could not be achieved due to instabilities endemic to the unmodified ADM formulation.

Using excision in the BSSN formulation, several groups have evolved stationary, vacuum black hole spacetimes with and without spin for arbitrarily long times.⁴¹⁾ Long-term stability has also been achieved using hyperbolic formulations of the field equations⁴²⁾ and characteristic formulations.⁴³⁾ Excision has also been used to simulate the grazing collision of two black holes⁴⁴⁾ and binary black holes initially in circular orbit and remaining in orbit for approximately one orbital period.⁴⁵⁾

Some of the most recent advances involving black hole excision involve its incorporation in 3+1 BSSN relativistic hydrodynamics schemes that treat perfect gases,⁴⁶⁾ imperfect gases with viscosity⁷⁾ and GRMHD fluids.^{18),19)} In addition, black hole excision has been implemented in a new 3 + 1 scalar wave scheme in generalized harmonic coordinates that has been used to follow the plunge, merger and ringdown of a binary black hole system formed from the collapse of scalar waves.⁴⁾

§6. Relativistic Hydrodynamics With Viscosity

The advent of robust, new formulations of the 3 + 1 equations, like BSSN, now makes it possible to track the *secular* evolution of a relativistic star over many dynamical timescales. The implementation of black hole excision makes it possible to track the collapse of a radially unstable star for a time interval $\Delta t \gg M$ following the formation of a black hole. Both of these advances were recently exploited to

follow the long-term evolution of a hypermassive star driven radially unstable to collapse by the action of shear viscosity.⁷⁾ This treatment was essentially the first time that the tools of numerical relativity were employed to integrate the relativistic $3 + 1$ Navier-Stokes equations for an imperfect gas. The stress-energy tensor for an imperfect fluid containing viscosity is $T^{ab} = T_{\text{ideal}}^{ab} + T_{\text{visc}}^{ab}$, where T_{ideal}^{ab} is the familiar expression for an ideal gas and T_{visc}^{ab} is given by⁴⁷⁾

$$T_{\text{visc}}^{ab} = -2\eta\sigma^{ab} - \zeta\theta P^{ab} . \quad (6.1)$$

In eqn. (6.1), η is the shear viscosity, σ^{ab} is the shear tensor, ζ is the bulk viscosity, θ is the expansion and $P^{ab} = g^{ab} + u^a u^b$ is the projection tensor of the fluid, where u^a is the fluid 4-velocity. In the numerical simulations of hypermassive stars, the shear viscosity was chosen to be proportional to the gas pressure and the bulk viscosity was set equal to zero, since it is the shear viscosity that redistributes angular momentum. The magnitude of η , though enhanced, was chosen to maintain the inequality $t_{\text{visc}} \gg t_{\text{dyn}}$ between the viscous and dynamical timescales, thereby satisfying a physically realistic, but computationally challenging, timescale hierarchy. The viscosity heats up the fluid according to

$$\rho_0 T(ds/d\tau)_{\text{visc}} = 2\eta\sigma^{ab}\sigma_{ab} . \quad (6.2)$$

In Ref. 7), two extreme opposite cases are treated for the net cooling of the fluid (e.g, by electromagnetic radiation or neutrino emission): “no cooling”, appropriate whenever $t_{\text{cool}} \gg t_{\text{visc}}$, where t_{cool} is the thermal cooling timescale, and “rapid cooling”, appropriate when the inequality is reversed. In axisymmetry, the evolution can be tracked over dozens of rotation periods (thousands of M).

The key result is that viscosity operating in a hypermassive star generically leads to the formation of a compact, uniformly rotating core surrounded by a low-density disk (“viscous braking of differential rotation”). The core typically grows more massive in time, ultimately becoming unstable to gravitational collapse. The simulations can track the secular evolution of the star, its dynamical collapse to a black hole, and, using black hole excision, relaxation to a final, stationary, black hole-disk quasiequilibrium state. The masses and spins of the final black hole and ambient disk are in good agreement with the values inferred from an analytic estimate based on the stellar density and angular momentum profiles at the onset of collapse.⁴⁸⁾

One interesting finding is that, for a given viscosity law, the secular evolution exhibits a simple scaling behavior provided $t_{\text{visc}} \gg t_{\text{dyn}}$: the evolving matter profiles are identical, independent of the magnitude of the viscosity, except that the timescale for the matter to reach a certain state prior to collapse varies inversely with the viscosity, i.e., $t_2 = t_1(\eta_1/\eta_2)$.

Fig. 3 depicts the evolution without cooling of a hypermassive, $n = 1$ polytrope with $J/M^2 = 1$ that exceeds the maximum mass of a uniformly rotating polytrope with the same index by a factor of 1.47. Viscosity drives secular evolution, leading to catastrophic collapse and the formation of a rotating black hole containing 77% of the total initial rest mass and 35% of the initial spin ($J_h/M_h^2 \approx 0.5$) . The remainder of the rest mass and spin go into the ambient disk, which continues to accrete slowly

onto the black hole. Because the ambient disk has appreciable mass, the spacetime is not strictly Kerr. However, an ergoregion develops about hole, as well as an ISCO (innermost stable circular orbit); the ISCO is evident by tracking the gas flow in the equatorial plane near the black hole and noting the transition from secular inspiral to dynamical plunge.

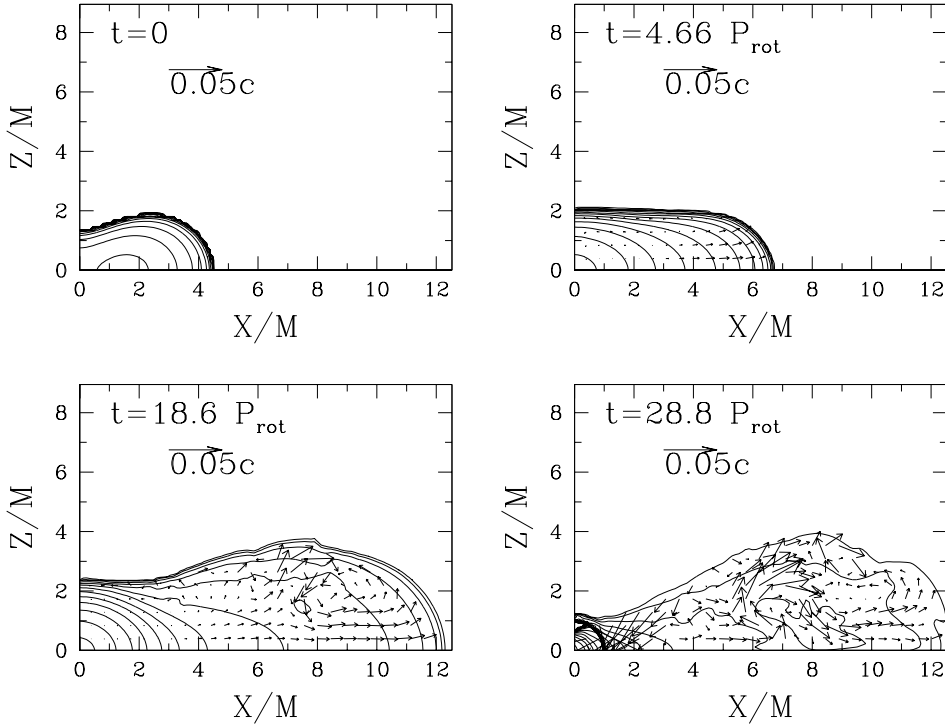


Fig. 3. Meridional rest-mass density contours and velocity field at select times (in units of central rotation period P_{rot}) for a hypermassive star with shear viscosity. The system is axisymmetric and experiences no cooling. The levels of the contours (from inward to outward) are $\rho_0/\rho_{0,\text{max}} = 10^{-0.15(2j+0.6)}$, where $j = 0, 1, \dots, 12$. In the lower right panel ($t = 28.8P_{\text{rot}}$), the thick curve denotes the apparent horizon. [From Duez et al. 2004.]

§7. Binary Black Hole – Neutron Stars

The first treatments of both the initial data and the evolution of BBHNSs that construct the combined BH-NS spacetime in a general relativistic framework have been presented recently. The initial data in these treatments consists of two stars in circular orbit and is constructed in the conformal thin-sandwich approximation by assuming that the spacetime possesses an approximate helical Killing vector. This condition is designed to yield a nearly stationary metric in the frame corotating with the orbit. Current implementations treat the regime $M_{\text{NS}}/M_{\text{BH}} \ll 1$.³⁾ Two distinct cases are considered for the conformally related background metric $\tilde{\gamma}_{ij}$: a Kerr-Schild BH metric and an isotropic (conformally flat) BH metric. Two opposite

limiting cases are considered for the NS spin, corotation and irrotation, for several different polytropic EOSs. The two background metrics give comparable values for the orbital angular velocity and the maximum stellar density at the Roche (tidal break-up) limit for the binaries. Any difference in these scalar invariants reflects the degree to which the physical models are sensitive to the assumed background metric; evolution calculations are required to interpret the differences.

Evolution calculations have been performed with the corotational, conformally flat, initial data, with the approximation that the spatial metric remains conformally flat.⁴⁹⁾ The matter is evolved using a relativistic Lagrangian smoothed particle hydrodynamics (SPH) scheme. The first simulations have been for neutron stars with low-compactness, $M_{\text{NS}}/R_{\text{NS}} = 0.04$, with $M_{\text{NS}}/M_{\text{BH}} = 0.1$. A radiation-reaction potential is included in the Euler equation to trigger the inward spiral (see Fig. 4).

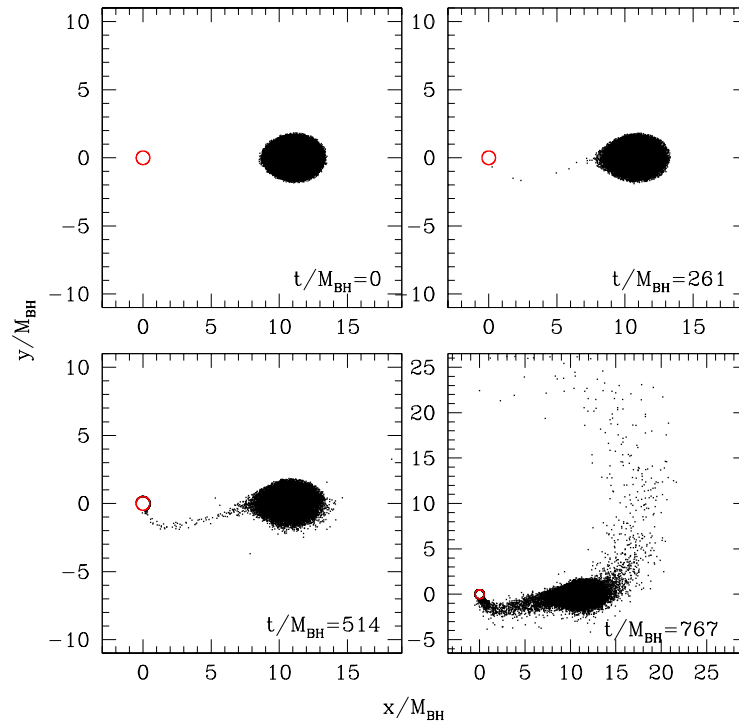


Fig. 4. Snapshots of SPH particle configurations projected into the orbital plane at select times corresponding to the initial configuration and 1, 2, and 3 full orbits, respectively. The BH horizon is shown as a circle at an isotropic radius $r = 0.5M_{\text{BH}}$. The binary separation begins just outside the Roche tidal radius. Radiation-reaction initially drives an inwardly directed mass-transfer stream onto the BH, until somewhere after $t/M_{\text{BH}} = 700$, when the expansion of the NS becomes unstable and tidal disruption occurs. [From Faber et al. 2005.]

These preliminary simulations show that mass transfer, when it begins while the neutron star orbit is still outside the BH ISCO, is more unstable than is typically predicted by analytical formalisms, i.e., $dM_{\text{NS}}/dt \gg M_{\text{NS}}/t_{\text{GW}}$, where t_{GW} is the gravitational wave inspiral timescale. This dynamical mass loss is found to be

the driving force in determining the subsequent evolution of the binary orbit and the neutron star, which typically disrupts completely within a few orbital periods. The majority of the mass transferred onto the black hole is accreted promptly; a significant fraction ($\sim 30\%$) of the mass is shed outward as well, some of which will become gravitationally unbound and ejected completely from the system. The remaining portion forms an accretion disk around the black hole, and could provide the energy source for short-duration gamma ray bursts. More detailed studies are underway.

§8. General Relativistic MHD

Magnetic fields play a crucial role in determining the evolution of many relativistic objects. In any highly conducting astrophysical plasma, a frozen-in magnetic field can be amplified appreciably by gas compression or shear. Even when an initial seed field is weak, the field can grow in the course of time to significantly influence the gas dynamical behavior of the system. In problems where the self-gravity of the gas can be ignored, simulations can be performed in a fixed background spacetime. Some accretion problems fall into this category. In many other problems, the effect of the magnetized fluid on the metric cannot be ignored, and the two must be evolved self-consistently. The final fate of many of these relativistic astrophysical systems, and their distinguishing observational signatures, may hinge on the role that magnetic fields play during the evolution. Some of these systems are promising sources of gravitational radiation, while others also may be responsible for gamma-ray bursts.

Examples of astrophysical scenarios involving strong-field *dynamical* spacetimes in which MHD effects may play a decisive role include the following:

- The merger of a BNS. The coalescence can lead to the formation of a hypermassive star supported by differential rotation, as discussed in Section 4. The growth of magnetic fields through magnetic braking (winding) and the magnetorotational instability (MRI) is alone sufficient to drive the star unstable, even if the seed magnetic field is small.^{24),50)} This process can lead to delayed collapse and massive disk formation, accompanied by a delayed gravitational wave burst.

- Core collapse in a supernova. Core collapse may induce differential rotation, even if the rotation of the progenitor at the onset of collapse is only moderately rapid and almost uniform. Differential rotation can wind up a frozen-in magnetic field to high values, at which point it may provide a significant source of stress, which could affect the explosion.⁵¹⁾

- The generation of gamma-ray bursts (GRBs). Short-duration GRBs are thought to result from BNS mergers,^{52),53)} or tidal disruptions of neutron stars by black holes,⁵⁴⁾ or hypergiant flares of ‘magnetars’ associated with the soft gamma-ray repeaters.⁵⁵⁾ Long-duration GRBs likely result from the collapse of rotating, massive stars which form black holes (‘collapsars’).⁵⁶⁾ In current scenarios, the burst is powered by the extraction of rotational energy from the neutron star or black hole, or from the remnant disk material formed around the black hole.⁵⁷⁾ Strong magnetic fields provide a likely mechanism for extracting this energy on the required timescale and driving collimated GRB outflows in the form of relativistic jets.⁵⁸⁾ Even if the

initial magnetic fields are weak, they can be amplified to the required values by differential motions.⁵⁹⁾

- Supermassive black hole (SMBH) formation. The cosmological origin of the SMBHs observed in galaxies and quasars is one of the key unsolved problems of structure formation in the early universe. Several hypotheses involve relativistic fluids in which magnetic fields can play an important role. It is thought that SMBHs start from smaller initial seed black holes, which grow to supermassive size by a combination of accretion and mergers. The seed black holes might be provided by the collapse of massive ($M \sim 10^2 M_\odot$) Population III stars.⁶⁰⁾ If so, magnetic forces can affect the collapse leading to the formation of these seeds, as well as their growth by accretion.⁶¹⁾ In fact, for Eddington-limited disk accretion, magnetic fields could be crucial to explaining how the growth of such seeds could be sufficiently rapid to account for the high SMBH masses inferred for the very youngest quasars.⁶²⁾ QSO SDSS 1148+5251, the quasar with the highest known redshift ($z = 6.43$) and believed to be powered by a SMBH that has grown to a mass $M \sim 10^9 M_\odot$, is a case in point. An alternative possibility is that SMBHs form directly from the catastrophic collapse of supermassive stars (SMSs).⁶³⁾ The evolution of a SMS may proceed differently, depending on whether the SMS rotates uniformly, in which case it ultimately undergoes collapse to a SMBH,⁶⁴⁾ or differentially, in which case it becomes unstable to a bar mode prior to reaching the onset of collapse.⁶⁵⁾ Magnetic fields and the turbulence they generate provide the principle mechanisms that damp differential rotation in SMSs,⁶⁶⁾ and thus such fields may determine their ultimate fate.

- The r-mode instability in rotating neutron stars. This instability has been proposed as a possible mechanism for limiting the angular velocities in neutron stars and producing observable quasi-periodic gravitational waves.⁶⁷⁾ However, preliminary calculations suggest that if the stellar magnetic field is strong enough, r-mode oscillations will not occur.⁶⁸⁾ Even if the initial field is weak, fluid motions produced by these oscillations may amplify the magnetic field and eventually distort or suppress the r-modes altogether. (R-modes may also be suppressed by non-linear mode coupling⁶⁹⁾ or hyperon bulk viscosity.⁷⁰⁾)

Several numerical codes which evolve the GRMHD equations on *fixed* Schwarzschild or Kerr black hole spacetimes have been developed in the past decade.⁷¹⁾ These codes have been used to study the structure of accretion flows onto Kerr black holes, the Blandford-Znajek effect in low-density regions near the hole, and the formation of GRB jets. Until very recently, little progress has been made to treat GRMHD flows in *dynamical* spacetimes beyond the earliest attempt thirty years ago by Wilson,⁷²⁾ who simulated the collapse of a rotating SMS with a frozen-in poloidal magnetic field in axisymmetry using a code that assumed the conformal flatness approximation for the spatial metric, thereby eliminating all gravitational radiation. In the past year a new code has been developed to evolve GRMHD fluids in dynamical spacetimes without approximation.¹⁸⁾ The code solves the Einstein-Maxwell-MHD system of coupled equations both in axisymmetry and in 3+1 dimensions. It evolves the metric by integrating the BSSN equations, and uses a conservative shock-capturing scheme to evolve the GRMHD equations. The contribution of the electromagnetic

field to the stress energy tensor in the GRMHD limit may be simply expressed as

$$T_{\text{em}}^{ab} = b^2 u^a u^b + \frac{1}{2} b^2 g^{ab} - b^a b^b, \quad (8.1)$$

where u^a is the fluid 4-velocity, $b^a = B^a/\sqrt{4\pi}$, $B^a = u_a F^{*ab}$ is the magnetic field measured by an observer comoving with the fluid, and F^{*ab} is the dual of the Faraday tensor. The code gives accurate results in standard GRMHD code-test problems, including magnetized shocks and magnetized Bondi accretion flow. To test the code’s ability to evolve the GRMHD equations in a dynamical spacetime, perturbations of a homogeneous, magnetized fluid (i.e. Alfvén waves, and both fast and slow magnetosonic waves) excited by a gravitational plane wave were studied, and good agreement between the numerical and new analytic solutions were found (see Fig. 5 and 6). This code has been followed by other robust codes that have been constructed in a similar fashion, also using the BSSN formalism.^{19),20)}

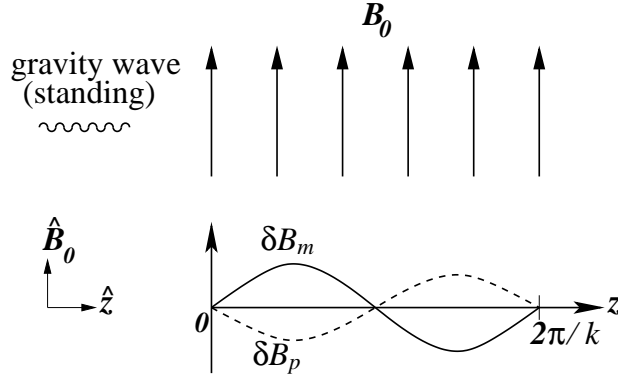


Fig. 5. Perturbation of the magnetic field $\delta\mathbf{B} = (\delta B_m + \delta B_p)\hat{\mathbf{B}}_0$ induced by a standing gravitational wave when $\mathbf{k} \cdot \mathbf{v}_A = 0$. The unperturbed magnetic field \mathbf{B}_0 is perpendicular to the wave vector of the gravitational wave $\mathbf{k} = k\hat{z}$. Both stationary modes δB_p and δB_m have the same $\sin kz$ spatial dependence, but they oscillate with different amplitudes and at different frequencies. [From Duez et al. 2005b]

This new computational tool will soon be applied to address some of the important astrophysical problems involving GRMHD that were listed earlier in this section. To preview such applications, the solution to the collapse of a perfectly conducting, homogeneous, spherical dust ball, initially at rest and threaded by a weak magnetic dipole field has been obtained recently (“magnetized Oppenheimer-Snyder collapse”).⁷³⁾ The solution applies in the limit $B^2/8\pi \ll M\rho/R$, where M is the mass, R is the radius and ρ is the density of the star. In this limit the matter and metric are unaffected by the electromagnetic field. Adopting this “dynamical Cowling approximation”, the electromagnetic field has been evolved both in the stellar interior and vacuum exterior. The interior solution is analytic while the exterior requires a numerical integration. Junction conditions were used to match the electromagnetic fields across the stellar surface. This model has proven useful to experiment with several gauge choices for handling spacetime evolution characterized by magnetized matter, the formation of a black hole and the associated appearance

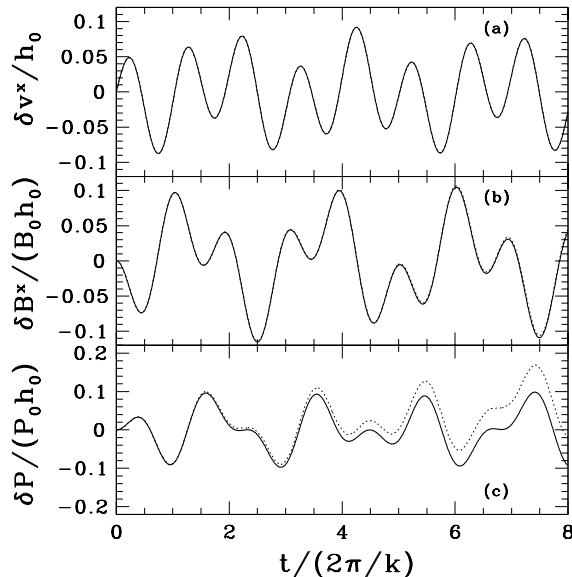


Fig. 6. Analytic and numerical solutions for the perturbations of a magnetized fluid due to the presence of a gravitational wave. The thick solid and thin dotted lines represent, respectively, the analytic and numerical solutions, though the two lines are not readily distinguishable in plots (a) and (b). All quantities are evaluated at $kz = \pi/4$ and are normalized as indicated. Time is normalized by the gravitational wave period. The drift noticeable in the pressure perturbation is not due to numerical error, but to nonlinear contributions neglected in the analytic solution. [From Duez et al. 2005a.]

of a spacetime singularity. These choices ranged from “singularity avoiding” time coordinates, like maximal time-slicing, to “horizon penetrating” time coordinates, like Kerr-Schild time-slicing, accompanied by black hole excision. The virtue of the later choice is that it allows the integration of the exterior electromagnetic fields to proceed arbitrarily far into the future (see Figs 7 and 8). At late times the longitudinal magnetic field in the exterior transforms into a transverse electromagnetic wave; part of the electromagnetic radiation is captured by the hole and the rest propagates outward to large distances. The asymptotic dipole electromagnetic field in the exterior vacuum is found to decay away with time as $t^{-(2l+2)}$, where $l = 1$, in accord with Price’s theorem.⁷⁴ This solution will be used to compare with forthcoming solutions generated by the new GRMHD codes that will treat more realistic collapse scenarios. It will be particularly interesting to see how the solutions will differ when the star is rotating and when the exterior region consists of a low-density, conducting atmosphere instead of a vacuum.

Simulations using the new GRMHD codes to evolve magnetized hypermassive stars, magnetized stellar collapse, and the black hole - ambient disk systems they produce are now underway. They should provide definitive answers to long-standing questions regarding the behavior and ultimate fate of these systems, which seem to arise in so many astrophysical contexts.

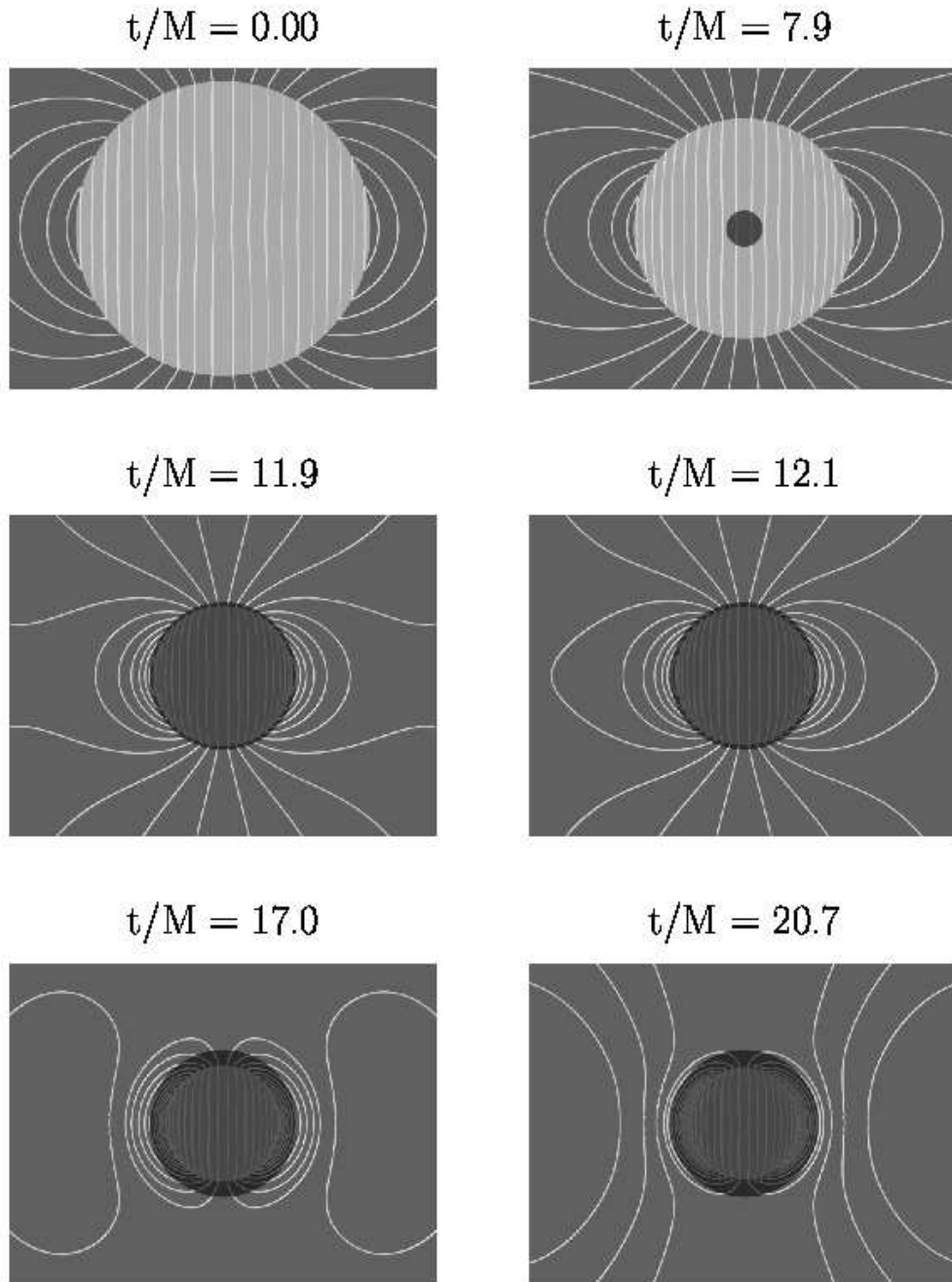


Fig. 7. Snapshots of the interior and exterior magnetic field lines on select *maximal* time slices. The star collapses from rest at an initial areal radius $R_s(0) = 4M$. The light shaded sphere covers the matter interior; the black shaded sphere covers the region inside the event horizon. In this gauge the stellar surface approaches a limit surface at $r_s \approx 1.5M$ at late times. The horizon grows to its final value $r_s = 2M$ once all the matter crosses inside this radius. Soon after the last snapshot at $t = 20.7$ grid stretching causes the quality of the numerical integration to deteriorate in this gauge. [From Baumgarte and Shapiro 2003b.]

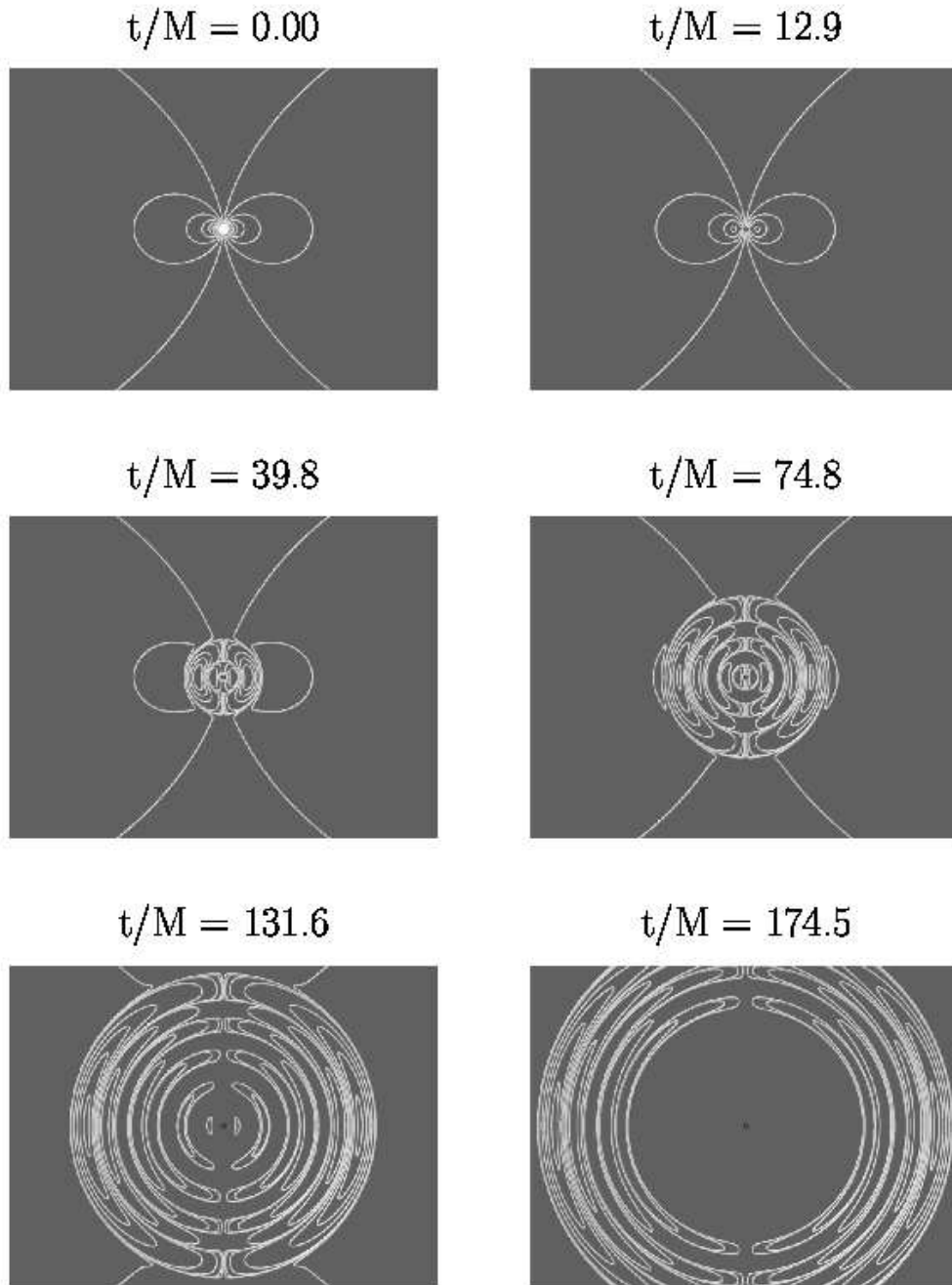


Fig. 8. Snapshots of the exterior magnetic field lines at select *Kerr-Schild* time slices for the same collapse depicted in Fig. 7. The white shaded sphere covers the matter interior; the black shaded area covers the region inside the event horizon; the grey shaded area covers the region inside $r_s = M$ excised from the numerical grid once the matter passes inside. In this gauge, using excision, we are able to integrate reliably to arbitrary late times. Note the transformation of the dipole magnetic field from a quasi-static longitudinal to a transverse electromagnetic wave. [From Baumgarte and Shapiro 2003b.]

Acknowledgements

We would like to thank T. Baumgarte, M. Duez, J. Faber, C. Gammie, Y.-T. Liu, M. Shibata, B. Stephens, and K. Taniguchi for useful discussions. This work was supported in part by NSF grants PHY-0205155 and PHY-0345151 and NASA Grant NNG04GK54G at the University of Illinois.

References

- 1) T. W. Baumgarte and S. L. Shapiro, Phys. Rept., **376** (2003), 41.
- 2) M. Shibata, K. Taniguchi and K. Uryu, Phys. Rev. D **71** (2005), 084021; M. Shibata, Phys. Rev. Lett. **94** (2005), 201101.
- 3) T. W. Baumgarte, M. L. Skoge and S. L. Shapiro, Phys. Rev. D **70** (2004), 064040; K. Taniguchi, T.W. Baumgarte, J. A. Faber and S. L. Shapiro, astro-ph/0505450 (2005).
- 4) F. Pretorius, gr-qc/0507014, (2005).
- 5) M. Shibata, T. W. Baumgarte and S. L. Shapiro, Astrophys. J. **542** (2000), 453.
- 6) M. Saijo, M. Shibata, T. W. Baumgarte and S. L. Shapiro, Astrophys. J. **548** (2001), 919.
- 7) M. D. Duez, Y.-T. Liu, S. L. Shapiro and B. C. Stephens, Phys. Rev. D **69** (2004), 104030.
- 8) S. L. Shapiro and S. A. Teukolsky, Astrophys. J. **298** (1985), 34; Astrophys. J. **298** (1985), 58; Astrophys. J. Lett. **292** (1985), 41; Astrophys. J. **307** (1986), 575; Phil. Trans. R. Soc. Lond. A **340** (1992) 365.
- 9) F. A. Rasio, S. L. Shapiro and S. A. Teukolsky, Astrophys. J. **344** (1989), 146.
- 10) I. Olabarrieta and M. W. Choptuik, Phys. Rev. D **65** (2002), 024007.
- 11) S. L. Shapiro and S. A. Teukolsky, Phys. Rev. D **45** (1992), 2739
- 12) R. A. Matzner, E. Seidel, S. L. Shapiro, L. Smarr, W.-M. Suen, S. A. Teukolsky and J. Winicour, Science **270** (1995), 941.
- 13) E. Seidel and W.-M. Suen, Phys. Rev. Lett. **69** (1992), 1845.
- 14) M. W. Choptuik, Phys. Rev. Lett. **70** (1993), 9.
- 15) C. Gundlach, Phys. Rept. **376** (2003), 339.
- 16) S. L. Shapiro and S. A. Teukolsky, Phys. Rev. Lett. **66** (1991), 994; E. W. Hirschmann and D. M. Eardley, Phys. Rev. D **51** (1995), 4198; R. Hamadé and J. M. Stewart, Class. Quantum Grav. **13** (1996), 497; B. K. Berger, Living Rev. Relativity, 2002, 1, gr-qc/0201056.
- 17) T. W. Baumgarte and S. L. Shapiro, Astrophys. J. **585** (2003), 921.
- 18) M.D. Duez, Y.-T. Liu, S. L. Shapiro, B. C. Stephens, Phys. Rev. D **72** (2005), 024028; Phys. Rev. D **72** (2005), 024029.
- 19) M. Shibata and Y. Sekiguchi, Phys. Rev. D **72** (2005), 044014.
- 20) L. Anton, O. Zanotti, J. A. Miralles, J. M. Martí, J. M. Ibanez, J. A. Font, J. A. Pons, astro-ph/0506063 (2005).
- 21) R. Arnowitt, S. Deser and C. W. Misner in *Gravitation: An Introduction to Current Research*, ed. L. Witten (Wiley, New York, 1962).
- 22) M. Shibata and T. Nakamura, Phys. Rev. D **52** (1995), 5428; T. W. Baumgarte and S. L. Shapiro, Phys. Rev. D **59** (1999), 024007.
- 23) A. Lichnerowicz, J. Math. Pure Appl. **23**, (1944), 37; J. W. York, Jr, Phys. Rev. Lett. **26** (1971), 1656.
- 24) T. W. Baumgarte, S. L. Shapiro and M. Shibata, Astrophys. J. Lett. **528** (2000), 29.
- 25) I. A. Morrison, T. W. Baumgarte and S. L. Shapiro, Astrophys. J. **610** (2004), 941.
- 26) J. R. Wilson and G. J. Mathews in *Frontiers in Numerical Relativity*, ed. C. Finn and L. Hobill (Cambridge University Press, Cambridge); J.W. York, Jr., Phys. Rev. Lett. **82** (1999), 1350; G. B. Cook, Living Rev. Rel. **5**, (2000), 1.
- 27) T. W. Baumgarte, G. B. Cook, M. A. Scheel, S. L. Shapiro, and S. A. Teukolsky, Phys. Rev. Lett. **79** (1997), 1182 and Phys. Rev. D **57** (1998), 7299; E. Gourghoulhon, P. Grandclément, K. Taniguchi, J.-A. Marck, and S. Bonazzola, Phys. Rev. D **63** (2001), 064029.
- 28) S. Bonazzola, E. Gourghoulhon and J.-A. Marck, Phys. Rev. Lett. **82** (1999), 892; P. Maronetti, G. J. Mathews, J. R. Wilson, Phys. Rev. D **60** (1999), 087301; K. Uryu and Y. Eriguchi, Phys. Rev. D **61** (2000), 124023; K. Taniguchi and E. Gourghoulhon, Phys. Rev. D **66** (2000), 104019.

- 29) C. A. Kochanek, *Astrophys. J.* **398** (1992), 234; L. Bildsten and C. Cutler, *Astrophys. J.* **400** (1992), 175.
- 30) M. Shibata, K. Taniguchi and K. Uryu, *Phys. Rev. D* **68** (2003), 084020.
- 31) S. E. Thorsett and D. Chakrabarty, *Astrophys. J.* **512** (1999), 288; I. H. Stairs, *Science*, **304**, (2004), 547.
- 32) F.A. Rasio and S. L. Shapiro, *Astrophys. J.* **432** (1994), 242; *Class. Quantum Grav.*, **16**, (1999), 1; X. Zhuge, J. M. Centrella, and S. L. McMillan, *Phys. Rev. D* **54** (1996), 7261.
- 33) J. A. Faber and F. A. Rasio, *Phys. Rev. D* **62** (2000), 064012; **65**, 2002, 08402.
- 34) J. A. Faber, P. Grandclément, F. A. Rasio, *Phys. Rev. D* **69** (2004), 124036.
- 35) D. J. Nice, E. M. Splaver, I. H. Stairs, O. Loehmer, A. Jessner, M. Kramer, J. M. Cordes, submitted to *Astrophys. J.*, (astro-ph/0508050).
- 36) W. Unruh, as cited in J. Thorneburg, *Class. Quantum Grav.*, **4**, (1987), 1119.
- 37) R. L. Marsa and M. W. Choptuik, *Phys. Rev. D* **54** (1996), 4929; P. Anninos *et. al.*, *Phys. Rev. D* **51** (1995), 5562; R. Gómez, R. Marsala, and J. Winicour, *Phys. Rev. D* **56** (1997), 6310.
- 38) M. A. Scheel, S. L. Shapiro and S. A. Teukolsky, *Phys. Rev. D* **51** (1995), 4208; **51**, (1995), 4236.
- 39) P. Anninos, K. Camarda, J. Massó, E. Seidel, W.-M. Suen and J. Towns, *Phys. Rev. D* **52** (1995), 2059.
- 40) Binary Black Hole Grand Challenge Alliance, *Phys. Rev. Lett.* **80** (1998), 2512.
- 41) M. Alcubierre and B. Brügmann, *Phys. Rev. D* **63** (2001), 104006; H.-J. Yo, T. W. Baumgarte and S. L. Shapiro, *Phys. Rev. D* **66** (2002), 084206.
- 42) M. A. Scheel, L. E. Kidder, L. Lindblom, H. P. Pfeiffer, and S. A. Teukolsky, *Phys. Rev. D* **66** (2002), 124005; G. Calabrese *et. al.* *Class. Quantum Grav.*, **20**, (2003), L245; M. Tiglio, L. Lehner and D. Neilsen, *Phys. Rev. D* **70** (2004;104018;)
- 43) R. Gómez, L. Lehner, R. Marsa, and J. Winicour, *Phys. Rev. D* **57** (1998), 4778.
- 44) S. R. Brandt *et. al.*, *Phys. Rev. Lett.* **85** (2000), 5496.
- 45) B. Brügmann, W. Tichy and N. Jansen, *Phys. Rev. Lett.* **92** (2004), 21101.
- 46) M. D. Duez, S. L. Shapiro and H.-J. Yo, *Phys. Rev. D* **69** (2004), 104016; L. Baiotti *et al.*, *Phys. Rev. D* **71** (2005), 024035.
- 47) C. W. Misner, K. S. Thorne and J. A. Wheeler, *Gravitation*, (Freeman, San Francisco, 1973), p.567.
- 48) S. L. Shapiro and M. Shibata, *Astrophys. J.* **577** (2002), 904.
- 49) J. A. Faber, T. W. Baumgarte, S. L. Shapiro, K. Taniguchi and F. A. Rasio, submitted to *Phys. Rev. D*, 2005.
- 50) S. L. Shapiro, *Astrophys. J.* **544** (2000), 397; J. N. Cook, S. L. Shapiro and B. C. Stephens, *Astrophys. J.* **599** (2003), 1272; Y.-T. Liu and S. L. Shapiro, *Phys. Rev. D* **69** (2004), 044009.
- 51) J. M. LeBlanc and J. A. Wilson, *Astrophys. J.* **161** (1970), 541; S. Akiyama, J. C. Wheeler, D. L. Meier and I. Lichtenstadt, *Astrophys. J.* **584** (2003), 954; T. Takiwaki, K. Kotake, S. Nagataki and K. Sato, *Astrophys. J.* **616** (2004), 1086.
- 52) R. Narayan, B. Paczynski and T. Piran, *Astrophys. J. Lett.* **395** (1992), 83.
- 53) W. Kluźniak and M. Ruderman, *Astrophys. J. Lett.* **505** (1998), 113.
- 54) M. Ruffert and H.-J. Janka, *Astron. Astrophys.* **344** (1999), 573.
- 55) E. Nakar, A. Gal-Yam, T. Piran and D. B. Fox, astro-ph/0502148 (2005).
- 56) A. MacFadyen and S. E. Woosley, *Astrophys. J.* **524** (1999), 262.
- 57) N. Vlahakis and A. Königl *Astrophys. J. Lett.* **563** (2001), 129.
- 58) P. Mészáros and M. J. Rees *Astrophys. J. Lett.* **482** (1997), 29; T. Piran *Phys. Rept.* **314** (1999), 575.
- 59) H. C. Spruit, *Astron. Astrophys.* **349** (1999), 189; S. A. Balbus and J. F. Hawley, *Rev. Mod. Phys.*, **70** (1998), 1.
- 60) P. Madau and M. J. Rees, *Astrophys. J. Lett.* **551** (2001), 27.
- 61) C. F. Gammie, S. L. Shapiro and J. C. McKinney, *Astrophys. J.* **602** (2004), 312.
- 62) S. L. Shapiro *Astrophys. J.* **620** (2005), 59.
- 63) M. J. Rees, *Ann. Rev. Astron. Astrophys.*, **22** (1984), 471; T. W. Baumgarte and S. L. Shapiro, *Astrophys. J.* **526** (1999), 941.
- 64) M. Shibata and S. L. Shapiro, *Astrophys. J. Lett.* **572** (2002), 39.
- 65) K. C. B New and S. L. Shapiro, *Astrophys. J.* **548** (2001), 439.

- 66) Y. B. Zel'dovich and I. D. Novikov, *Relativistic Astrophysics, Vol I: Stars and Relativity*, (University of Chicago Press, Chicago, 1971).
- 67) N. Andersson, *Astrophys. J.* **502** (1998), 708; J. L. Freidman and S. Morsink, *Astrophys. J.* **502** (1998), 714.
- 68) L. Rezzolla, F. K. Lamb, D. Markovic and S. L. Shapiro, *Phys. Rev. D* **64** (2001), 104013; *Phys. Rev. D* **65** (2002), 024001.
- 69) A. K. Schenk, P. Arras, E. E. Flanagan, S. A. Teukolsky and I. Wasserman, *Astrophys. J.* **591** (2003), 1129; P. Gressman, L. M. Lin, W.-M. Suen, N. Sterigoulas and J. L. Friedman, *Phys. Rev. D* **66** (2002), 041303R.
- 70) P. B. Jones, *Phys. Rev. Lett.* **86** (2001), 1384; L. Lindlbom and B. J. Owen *Phys. Rev. D* **65** (2002), 063006.
- 71) M. Yokosawa, *Publ. Astron. Soc. Japan* **45**, (1993), 207; S. Koide, K. Shibata and T. Kudoh, *Astrophys. J.* **522** (1999), 727; J.-P. De Villiers and J. F. Hawley, *Astrophys. J.* **589** (2003), 458; C. F. Gammie, J. C. McKinney and G. Tóth, *Astrophys. J.* **589** (2003), 444; S. .S. Komissarov, *Mon. Not. R. Astron. Soc.* **350**, (2004), 1431
- 72) J. R. Wilson, *Ann. New York Acad. Sci.* **262**, (1975), 123.
- 73) T. W. Baumgarte and S. L. Shapiro, *Astrophys. J.* **585** (2003b), 930.
- 74) R. H. Price, *Phys. Rev. D* **5** (1972a), 2419; *Phys. Rev. D* **5** (1972b), 2439.